Functional properties of chitosan films modified by snail mucus extract

FUNCTIONAL PROPERTIES OF CHITOSAN FILMS MODIFIED BY SNAIL MUCUS EXTRACT

Maria Francesca Di Filippo[a], Silvia Panzavolta*[a], Beatrice Albertini[b], Francesca Bonvicini[c], Giovanna Gentilomi[c], Ramona Orlacchio[a], Nadia Passerini[b], Adriana Bigi[a], Luisa Stella Dolci[b]

[a]Department of Chemistry "G. Ciamician", University of Bologna, Via Selmi 2, 40126, Italy;

[b]Department of Pharmacy and BioTechnology, University of Bologna, Via S. Donato 19/2, 40127, Italy;

[c]Department of Pharmacy and Biotechnology, University of Bologna, Via Massarenti 9,40138, Italy

*Corresponding author: Silvia Panzavolta

Dipartimento di Chimica "G. Ciamician"
via Selmi 2 40126 Bologna (Italy)
tel +39 051 2099566
fax +39 051 2099456

silvia.panzavolta@unibo.it

Abstract

Snail mucus is an attractive natural substance, which is increasingly used in cosmetic creams and syrups thanks to its emollient, moisturizing, protective and reparative properties. The aim of the present study was to explore the physicochemical properties of chitosan-based films added with snail mucus extracted from *Helix Aspersa Muller*. To this aim, chitosan films at different content of snail mucus were fabricated by simple solvent casting technique. The results of X-ray diffraction analyses, tensile mechanical tests, Infrared spectroscopy and thermogravimetry demonstrated that snail mucus addition strongly modifies the properties of chitosan films. In particular, it acted like a plasticizer enhancing films extensibility up to ten times and strongly improving their water barrier and bioadhesion properties, with a trend depending on Snail mucus content. Furthermore, it

provides the films with antibacterial properties and enhanced cytocompatibility, yielding materials with tailored properties for specific requirements.

Keywords

Chitosan films; snail mucus; adhesive properties

1. Introduction

The environmental problems caused by the continuous increase of plastic pollution have stimulated many efforts addressed to find suitable substitutes obtained from natural and renewable sources through green processes [1]. Chitosan has been proposed as an eligible material with potential applications in many fields, including medicine, agriculture, food, textile, environment, and bioengineering, due to its excellent properties of nontoxicity, biocompatibility, biodegradability, chelating capability [2-5].

In particular, chitosan ability to form films has been widely exploited for food packaging [6], wound dressing and drug delivery applications [7-11]. Chitosan is a natural linear amino polysaccharide made of D-glucosamine and N-acetyl-D-glucosamine units. It is obtained by deacetylation of chitin, which is the structural component of the crustacean's shell (mostly shrimps and crabs), insect cuticles and fungi cell walls, and represents the second most abundant natural polymer after cellulose [12]. Chitosan is soluble in acid solutions due to the protonation of the $-NH_2$ groups on the C-2 position of the D-glucosamine repeat unit: as a consequence, the polysaccharide is converted to a polyelectrolyte in acidic media. DA, molecular weight and distribution of the acetyl groups along the main chain are determinant factors in chitosan properties [13-15]. In particular, the positive charge of the amino groups in acidic pH is considered responsible for the antimicrobial activity of chitosan, through the interaction with the negatively charged cell membranes of microorganisms [7].

A number of studies have been focused to modify composition and properties of chitosan-based films in order to improve their performance and widen their application fields. In particular, films with improved light barrier and extra protective shield against oxidative processes were produced by incorporation of compounds of natural origin as antioxidant and/or antimicrobial agents [16-20]. Addition of propolis was shown to enhance mechanical strength, antibacterial activity and antioxidant capacity of chitosan-based materials for food packaging applications [21].

Among natural-derived active substances, snail mucus is receiving a great deal of attention, as it has been recently proposed as an ingredient of several cosmetic (e.g. creams) and parapharmaceutical products for the management of wound and for the treatment of chronic bronchitis [22-23]. In fact, the mucus is an adhesive, emollient, moisturizing, lubricating and protective material, containing bioactive substances which are responsible for its unique properties not replicable in the laboratory with synthetic chemical compounds [24]. Moreover, in vitro assays on fibroblast cultures showed that snail mucus from Helix Complex does not elicit cytotoxicity, protects cells from apoptosis, promotes cell proliferation and migration, and displays antimicrobial activity [24]. However, despite the wide use of snail mucus in commercial products, the number of studies on the characterization of this animal-derived extract is still limited [25-30] and the articles investigating the properties of snail-mucus based composite materials are even less [31].

In this study we investigated the modifications of the properties of chitosan-based films induced by Snail mucus extract (S) obtained by MullerOne extraction method. Recently, we patented the application [32] of snail mucus extract on different polymer-based films, demonstrating that tensile behavior and adhesive properties greatly improved by increasing the S content, thus producing materials able for applications in pharmaceutic, veterinary and cosmetics fields (patent application n. 102019000004940). To this aim, we added different amounts of Snail extract to chitosan previously solubilized in acetic acid or in lactic acid. Moreover, the acidic character of S allowed the preparation

of a further series of films obtained by solubilizing chitosan directly in S solution. Films were then fully characterized for their solid-state properties, cell viability and antibacterial activity.

2. Materials and Methods

2.1 Materials

Chitosan (degree of deacetylation ≥ 93%, M.W.= 100 KDa) was purchased from Faravelli, Milan, Italy. Snail mucus from *Helix Aspersa Muller* (kindly offered by "I Poderi" farm, Montemerano, Italy) was extracted by MullerOne method (http://www.mullerone.com/it/en/extraction-process) and stored at 4°C in a sealed polyethylene bottle until use. Analysis of Snail mucus was obtained from the supplier and reported in table S1. Selected amounts of Snail mucus were also freeze-dried for 24 h to evaluate the amount of the dispersed components and stored at 4°C.

Acetic acid and lactic acid were purchased from Sigma Aldrich (Milan, Italy).

2.2 Preparation of Chitosan films

Chitosan films (1% w/v) were prepared by dissolving the proper amount of pure chitosan in either acetic acid (A, 1% v/v), or lactic acid (L, 1% v/v), as reported in literature, or directly in S. The mixture was kept at room temperature under stirring until complete dissolution of the polymer. A volume corresponding to 11 mL of this solution was poured in polyethylene Petri dishes (Ø= 5 cm) and put under laminar hood at room temperature overnight. The obtained films were labeled C_A, C_L and C_S, respectively.

2.3 Preparation of Chitosan-Snail mucus films

For both C_A and C_L solutions, two chitosan-snail mucus volume ratios were selected: 70:30 and 30:70, where the first number refers to the relative volume of chitosan acidic solution and the

second one to the volume of S with respect to the total volume. For example, 100mL of chitosan-S blend 70:30 were obtained by adding 1g of chitosan to 70mL of A (1% v/v) or L (1% v/v). The mixture was stirred at room temperature until complete dissolution of the polymer and then 30mL of S were added (30% of the final volume). After 2h of stirring, 11 mL of this solution were poured in each Petri dish and put under laminar hood overnight. The obtained films were labeled CA_7030 and CL_7030, respectively.

The films obtained with the chitosan:S volume ratio of 30:70 were labeled CA_3070 and CL_3070.

In order to obtain a chitosan-based film using the S as acidic medium, the same procedure was used: 1g of Chitosan was dissolved in 70 or 30mL of S and then 30 or 70mL of distilled water were added in order to obtain the films labeled CS_7030 and CS_3070, respectively.

Films were stored at room temperature between two sheets of plastic-coated aluminum closed inside PVC bags.

2.4 Films Characterization

2.4.1 Thickness

Films thickness was measured using a hand-held digital micrometer (Mitutoyo, Japan) at six different positions in each specimen to an accuracy of 0.001 mm.

2.4.2 Mechanical properties

Tensile tests were performed on strip-shaped samples (40 mm long and 4 mm width) using a 4465 Instron dynamometer equipped with a 100 N load cell. Stress-strain curves were recorded at a crosshead speed of 5 mm/min by the software SERIE IX for Windows. Ten samples were tested for each composition.

2.4.3 Infrared spectroscopy

The Fourier transform infrared spectra were recorded using a Thermo Scientific Nicolet iS10 FTIR spectrometer equipped with an ATR sampling device that uses a Germanium diamond as element for internal reflection. Spectra were acquired at room temperature in absorbance mode from 2300 to 800 cm^{-1} with a resolution of 2 cm^{-1}.

2.4.4 Water Vapor Permeability (WVP)

WVP is the water vapor transmission rate through a flat film area induced by a vapor pressure between two surfaces under specific conditions of moisture and temperature and was measured using the ASTME96-93 method [33], slightly modified [34]. Films disks (Ø=2 cm) were glued using silicon on the opening of glass vials containing 2g of anhydrous $CaCl_2$. Weighted vials were placed in a glass desiccator containing saturated $Mg(NO_3)_2 \cdot 6H_20$ solution (75% RH at 25°C). The vials were weighted every day until constant weights were achieved (4 days). WVP was calculated as follows:

$$WVP\ (gs^{-1}m^{-1}Pa^{-1}) = \frac{\Delta W\, \chi}{\Delta t\, A\, \Delta P} \quad (1)$$

where $\Delta W/\Delta t$ is the amount of water gained per unit time of transfer, A is the exposed area of the samples (0.00020 m^2), ΔP is water vapor pressure difference between both sides of the film (1670 Pa at 25°C, table value) and χ is the film thickness. Samples were tested in triplicate.

2.4.5 X-Ray diffraction

X-ray diffraction patterns were carried out by means of a Philips X'Celerator diffractometer equipped with a graphite monochromator in the diffracted beam (2θ range from 4° to 50°, step size = 0,06680, 40s/step). CuKα radiation (40 mA, 40 kV, 1.54 Å) was used.

2.4.6 Thermogravimetric analysis (TGA)

TGA was carried out using a Perkin-Elmer TGA-7. Heating was performed in a platinum crucible in air flow (20 mL/min) at a rate of 10°C/min up to 800°C. Samples weights were in the range of 5–10 mg.

2.4.7 Adhesive strength

The in vitro evaluation of the bioadhesive properties of the films was performed using an Anton Paar modular compact rheometer MCR102, adapting the method reported in the literature [35]. Pig rind bought in a local butcher's shop was used as support for the adhesion tests. Pig rind disks (Ø=2.5 cm) were gently washed with detergent in order to remove fat and rinsed with Phosphate Buffer (PB, pH=7.4) and water repeatedly. Rind disks were glued on the disposable aluminum inferior support of the instrument. The film was allowed to adhere on the skin by wetting the pig rind with a fixed volume (40 µL) of PB and applying a gentle finger pressure for 1 minute. Subsequently, the upper plunger of the instrument, covered with double-sided tape (3M), was lowered until a force of 10 N was applied to the film for 30 seconds. After that, the plunger was raised up at a speed of 1 mm/s and data were collected by using the RheoCompass Software. Work of adhesion and peak detachment force were used to evaluate the bioadhesive strength of the films. Each formulation was analyzed in triplicate and the mean ± SD was reported.

2.4.8 Statistical analysis

Statistical analysis was performed with Graph Pad Prism 4. One-way analysis of variance (ANOVA) followed by Tukey's Multiple Comparison Test was employed to assess statistical significance of the experimental conditions for Water Vapor Permeability and Adhesive strength; statistically significant differences were determined at $p < 0.05$.

2.5 Cell viability bioassay

The effect of chitosan films on nonmalignant epithelial cells metabolism was assessed *in vitro* after incubation of disks (Ø= 6 mm) in 1 mL of Eagle's Minimal Essential Medium (MEM) at 37°C for 24h. Then, the media were used for the analysis on African green monkey kidney cells (Vero ATCC CCL-81). Briefly, cells were cultured in MEM supplemented with 10% fetal bovine serum (Carlo Erba Reagents, Milan, Italy), 100 U/mL penicillin and 100 µg/mL streptomycin at 37°C with 5% CO_2. For experiments, cells were seeded into 96-well plates at 10^4 cells/well, and incubated at 37 °C for 24 h; subsequently, cell monolayer was washed with PBS and incubated with 100 µL of the different solutions, previously diluted twenty times in cell culture medium. The cell viability was assessed by a WST8-based assay according to the manufacturer's instructions (CCK-8, Cell Counting Kit-8, Dojindo Molecular Technologies, Rockville, MD, USA). After 72 h of incubation, cell monolayer was washed with PBS, and 100 µL of fresh medium containing 10 µL of CCK-8 solution were added. After 2h at 37°C, the absorbance was measured at 450/630 nm; results were expressed as the percentage of absorbance relative to the untreated controls. Experiment was carried out in triplicate.

2.6 Antibacterial activity

The *in vitro* antibacterial activity of the chitosan films was evaluated against *Staphylococcus aureus* (ATCC 25923) and *Escherichia coli* (ATCC25922) selected as controls and representative strains for Gram-positive and Gram-negative bacteria. The effectiveness of samples to inhibits bacterial growth was assessed by a standardized Kirby-Bauer (KB) diffusion test on Mueller-Hinton agar plate and by measuring the bacterial-free zone around the disk-shaped samples (Ø = 6mm) after 24h of incubation at 37°C [36]. All experiments were performed on duplicate in different days.

3. Results and discussion

Films-forming solutions of chitosan in lactic or acetic acid are extensively reported in literature [37,38]. However, to the best of our knowledge, this is the first paper which reports the peculiar properties provided to chitosan films by the addition of Snail mucus obtained by MullerOne extraction. This method of extraction provides an acidic solution suitable for solubilization of chitosan, which needs pH values below 6 to dissolve. It follows that the use of S allows direct solubilization of chitosan through a 'green' procedure and provides materials where the good characteristics of chitosan are enriched by the peculiar properties of Snail mucus extract.

All the chitosan-based films appeared transparent, with color gradually turning to yellow on increasing the amount of Solution (Fig. 1). The SEM images of some chitosan films containing or not Snail mucus extract are reported as example in Fig.1: all the films revealed a smooth surface without uneven areas.

As a general consideration, the flexibility of the films and their adhesiveness increase with S volume, making difficult their detachment from Petri dishes.

As reported in Table 1, films thickness is significantly affected by the acid used for chitosan dissolution: the thickness increases from acetic to lactic acid films can be ascribed to the increasing dimensions of the counterion [39]. A significantly greater augmentation of the values of thickness occurs on increasing the S content, most likely as a consequence of the increasing amount of dry matter (dry matter content of S after lyophilization: 5% m/V). The influence of the nature and composition of the film forming solution on thickness is clearly shown by the results obtained for the C_S samples, where water addition does not significantly affect the values of thickness [40].

Table 1. Effect of S incorporation on chitosan-based films on thicknesses and mechanical properties.

SAMPLES	Thickness (mm)	σ_b (MPa)[a]	ε_b (%)[a]	E (MPa)[a]
C_L	0.076 ± 0.009	32 ± 4	4.0 ± 0.8	1200 ± 100
CL_7030	0.100 ± 0.006	7 ± 2	23 ± 8	170 ± 20
CL_3070	0.156 ± 0.007	1.4 ± 0.2	50 ± 10	46 ± 12
C_A	0.052 ± 0.020	40 ± 3	10 ± 3	1760 ± 300
CA_7030	0.096 ± 0.019	15 ± 4	13 ± 6	270 ± 100
CA_3070	0.118 ± 0.007	0.9 ± 0.1	138 ± 10	0.8 ± 0.1
C_S	0.199 ± 0.005	0,43 ± 0.2	163 ± 30	0,38 ±0,05
CS_7030	0.168 ± 0.021	1.1 ± 0.19	88 ± 7	1.4 ± 0.22
CS_3070	0.158 ± 0.010	8.6 ± 1.5	12 ± 4	301 ± 44

[a]Each value is the mean of ten determinations and is reported with its standard deviation.

The results of mechanical characterization are summarized in Table 1. Both C_L and C_A films are rigid and brittle with high values of elastic modulus (E) and stress at break (σ_b), whereas C_S films exhibit a relatively high extensibility (ε_b) and low values of E and σ_b. In agreement, S addition to C_L and C_A compositions greatly influences the mechanical properties of the films, as clearly shown in Fig.2: ε_b increases with S content while σ_b and E decrease. The same trend is observed on going from CS_3070 to CS, in agreement with the increase of S content. The effect produced by S addition is similar to that obtained by the introduction of plasticizers into the composition of chitosan films [41-43]. The increased extensibility of the films at higher S concentration can be attributed to Solution–polymer interactions, which reduce the intermolecular interactions between polymer chains, facilitating their sliding and mobility and improving the overall extensibility.

The increased mobility of the polymer chains usually promotes also water vapor permeability (WVP) [43], that is the ease of moisture for penetrating and passing through the hydrophilic portion of film [44]. However, in our samples we found a peculiar trend as a function of composition (Fig. 3) since CA_7030 and CL_7030 exhibit WVP values significantly smaller than the other films of the series.

Interestingly, C_S films exhibit lower permeability than C_L and C_A films (*p<0.05). Moreover, the WVP values of C_S films are not significantly affected by water addition.

As stated previously, the films become sticky after addition of S: the adhesive properties, expressed in terms of force needed for film detachment (F) and work of adhesion (W), are reported in Fig. 4. C_A films do not exhibit any adhesive performance. However, the addition of S induces a certain adhesiveness, requiring a force up to about 10 N (CA_3070) to detach the films. A similar trend is observed for films prepared in lactic acid: C_L exhibits an appreciable adhesive behavior, which is further enhanced by S addition. As expected, the highest adhesive properties are recorded for films prepared by direct solubilization of chitosan into S Solution. The increased flexibility and adhesion of S-containing films should improve the contact with skin, thus allowing a better penetration of film components into the tissue. Besides, the presence of polar groups into Solution, most probably belongings to glycolic acid, allantoin and proteins (see Table S1) could increase the interactions.

Structural characterization

According to the literature, a number of crystalline polymorphs are known for chitosan; the most represented ones are an anhydrous form indicated as “annealed polymorph” and two different hydrated forms named “tendon” and “Type II” [45,46].

The variety of polymorphs is due to the presence of water molecules, which play an important role in the packing, conformation and mechanical properties of chitosan-based films. In hydrated forms, the chitosan structure can be stabilized by several hydrogen bonds between -N-H groups and water molecules. In addition, the crystalline structure of chitosan is strongly dependent on its processing treatment, as well as on its origin and molecular composition, such as degree of deacetylation and molecular weight [47].

The X-ray diffraction patterns collected from chitosan films are reported in Fig.5: films obtained in acetic acid (C_A) show two prominent reflections at about 9.2° and 12°/2θ, together with a sharp peak at 19°/2θattributed to type II hydrated polymorph of chitosan acetate [48]. Snail mucus is a complex mixture of active ingredients and it is not easy to discriminate the effectiveness and the interaction of each component with the chitosan functionalities. However, the comparison of the patterns collected from Solution-containing samples puts into evidence that the material becomes less crystalline on increasing the S content. In fact, CA_7030 films show only two broad halos, centered at about 8° and 20° of 2θ, while only a broad halo centered at 20° of 2θ can be detected when the samples contain a greater amount of solution (CA_3070). The X-ray pattern of the chitosan films obtained in lactic acid (C_L), reported in Fig. 5, evidences a poorly crystalline structure, with two broad reflections at about 6° and at about 20°/2θ.

S addition provokes an overall decrease of the intensity of the diffraction patterns. It can be hypothesized that, on S addition, chitosan-Solution interactions outweigh chitosan-chitosan interactions, leading to loss of structural order and, consequently, to the observed significant reduction in crystallinity. In agreement, the XRD patterns of all the samples of the C_S series display just a very broad halo centered at about 20° of 2θ.

In agreement with the X-rays patterns, the infrared absorption spectrum of C_A films displays a number of bands which can be ascribed to the hydrated polymorph of chitosan [49]. In particular, the absorption band at about 1640 cm^{-1} can be assigned to the C=O stretching (amide I), whereas those centered at about 1540 and 1390 cm^{-1}can be attributed to N-H bending (amide II) and C-N stretching, respectively [10]. Addition of S solution provokes a general broadening of the spectra, which assume characteristic features of the spectrum of S powder (see Fig.5), where an intense absorption peak, probably due to the high content of allantoin and glycolic acid in the solution (see Table S1), appears at around 1712 cm^{-1}. This absorption band also appears in the spectra of

composite films and its intensity increases on increasing S content. The resolution of the absorption bands centered at about 1072 cm^{-1}, associated to C-O stretching, decreases on increasing S content, suggesting interactions between the hydroxyl groups of chitosan and polar groups of S through hydrogen bonds [10]. By comparing IR spectrum of S with that reported in literature [24] it is clear that Snail extract obtained by MullerOne contains a minor amount of proteins (see also table S1) with respect to that obtained by a different method of extraction. We hypothesize that the use of ozone during snail stimulation should induce a partial protein degradation, thus lowering the proteic component of the final exctract.

In agreement with XRD results, the infrared absorption spectrum of C_L films is quite different and resembles those reported in literature for chitosan films prepared in lactic acid [50]. Addition of S to C_L films has a similar effect to that observed on C_A films, and the spectra are similar to those recorded for the C_S series.

The thermal stability of chitosan films was assessed by TGA analysis in air. Results obtained for the different films are reported in Figure 6 together with the thermal behavior of lyophilized S. C_A films display three steps of thermo-oxidative degradation [51]. The first one, in the temperature range 35–160°C, is attributed to the loss of absorbed water. The second one, between 160°C and 460°C and centered around 310°C, corresponds to the chemical degradation and deacetylation of chitosan [52], while the third step, in the temperature range 460–700°C, can be associated with the oxidative degradation of the carbonaceous residue formed during the second step. The thermogravimetric plot of C_L differs from that of C_A in the first region, which shows two distinct weight losses in the range 37-240°C, in agreement with the different structures evidenced by XRD and FT-IR data. The derivative plot of TGA (DTG) of freeze-dried S (Fig. 6) displays a weight loss centered at 190°C, which accounts for about 70% wt of weight loss, and further degradation steps between 300 and 800°C, probably due to the degradation of residues. A very similar thermogravimetric plot is shown by C_S,

with just some shift of the degradation steps to higher temperatures. Water addition (CS_7030 and CS_3070) causes just a reduction of the relative amount of the first weight loss. When S is added to the composition of C_A and C_L, all the films display similar thermogravimetric plots to that of C_S series: in particular, the thermal degradation starts at a temperature lower than that of pure chitosan films and the first mass loss, determined between 37°C and 300°C, accounts for about 35% wt and 48% wt for the 7030 and 3070 compositions, respectively. Moreover, no water loss was observed between 35°C and 160°C.

Biological properties

In our experimental conditions C_L and C_A films did not interfere with Vero cells metabolism after 72h of incubation (93.7% and 103.3 %, respectively, and relative to untreated control cells) (Fig. 7). Addition of snail mucus components to these films induced an improvement in cell viability, especially for the samples of CA series. These samples exhibit a dose dependent increase in Vero viability as function of S content. The lowest cell viability was detected for C_S films (72.7%); nevertheless, as a material is considered cytotoxic when its viability is less than 70% in comparison to untreated controls [53], all samples displayed a promising safety profile.

The antibacterial properties of the different chitosan films were evaluated *in vitro* by means of a disk agar diffusion method where inhibition of bacterial growth is demonstrated by the clear bacterial-free zone around sample disks following a 24 h-incubation. Results are reported in Table 2. There was no difference between the antibacterial effects on the different microbial species.

Although it is generally recognized that chitosan solutions have strong antibacterial activities [54], chitosan films did not inhibit bacterial growth in agar diffusion tests because chitosan in a film form is unable to diffuse through the surrounding agar media [55]. the present results confirm this feature since both C_A and C_L samples did not inhibit bacterial growth. As a consequence, the bacterial-

free zones observed for S-containing films could be definitely ascribed to snail mucus addition. Chitosan films prepared in acetic acid and directly in S showed antibacterial activity at the highest S content (CA_3070, C_S and CS_7030) confirming the inhibitory role of snail mucus. On the contrary, films prepared in lactic acid did not display antibacterial properties irrespective to S content.

Table 2. Ranges of the inhibition zone diameters (mm) measured for the chitosan films

Sample	*S. aureus* (ATCC 25923)	*E. coli* (ATCC 25922)
C_L	NA*	NA
CL_7030	NA	NA
CL_3070	NA	NA
C_A	NA	NA
CA_7030	NA	NA
CA_3070	12-13	11-12
C_S	15-22	11-14
CS_7030	15-16	12-13
CS_3070	NA	NA
GMN 10 μg	18-19	18-19

*NA; not appearing

4. Conclusion

New and highly versatile materials containing different amounts of snail mucus, obtained by MullerOne exctraction method, and chitosan have been obtained by simple solvent casting. The results of this work show that snail mucus can be added to chitosan previously solubilized in acetic or lactic acid, or it can also be used directly to dissolve chitosan trough a greener route. Tensile tests revealed that composite films can be stretched up more than ten times with respect to chitosan films, demonstrating that S addition displays a plasticizing effect on the films. Moreover, snail mucus also enhances water barrier properties and bioadhesion. Structural characterizations indicate that the interactions between snail mucus and chitosan chains involve hydrogen bonds between the hydroxyl groups of chitosan and polar groups of S, even if the complexity of the extract composition requires more detailed analysis. Thanks to the presence of S, composite films display enhanced cytocompatibility and significant antibacterial activity towards both Gram-positive and Gram-

negative bacteria. These results demonstrate that variations in composition can be utilized to modulate the properties of these materials for possible applications including those for the biomedical field or as edible coating for food packaging. However, due to the influence of the extraction methods on the snail extract properties, composite films made with different snail extract should be useful to get more information about the interactions between the components and to highlight the peculiar extract effect.

This research did not receive any specific grant from funding agencies in the public, commercial, or not-for-profit sectors.

REFERENCES

1) L.A. Andrady, Plastics and Environmental Sustainability, John Wiley & Sons, (2015).

2) M. Collado-González, Y. González Espinosa, F.M. Goycoolea, Interaction between chitosan and mucin: Fundamentals and Applications, Biomimetics (Basel), 4(2), (2019), doi: 10.3390/biomimetics4020032.

3) G.S. Dhillon, S. Kaur, S.J. Sarma, S.K. Brar, M. Verma, R.Y. Surampalli, Recent Development in Applications of Important Biopolymer Chitosan in Biomedicine, Pharmaceuticals and Personal Care Products, Curr. Tissue Eng., 2, (2013), pp. 20-40.

4) D. Nataraj, S. Sakkara, M. Meghwa, N. Reddy, Crosslinked chitosan films with controllable properties for commercial applications, Int. J. Biol. Macromol., 120, (2018), pp. 1256–1264.

5) H. Wang, J. Qian, F. Ding, Emerging Chitosan-Based Films for Food Packaging Applications, J. Agric. Food Chem., 66, (2018), pp. 395–413.

6) M. Mujtaba, R.E. Morsi, G. Kerch, M.Z. Elsabee, M. Kaya, J. Labidi, K.M. Khawar, Current advancements in chitosan-based film production for food technology; A review, Int. J. Biol. Macromol., 121, (2019), pp. 889–904.

7) Z. Shariatinia, Pharmaceutical applications of chitosan, Adv. Colloid Interface Sci., 263, (2018), pp. 131–194.

8) Q.X. Wu, D.Q. Lin, S.J. Yao, Design of Chitosan and Its Water Soluble Derivatives-Based Drug Carriers with Polyelectrolyte Complexes, Mar. Drugs, 12, (2014), pp. 6236-6253.

9) A.K. Sah, M. Dewangan, P.K. Suresh, Potential of chitosan-based carrier for periodontal drug delivery, Colloids Surf. B: Biointerfaces, 178, (2019), pp. 185–198

10) I. Laceta, P. Guerrero, K. de la Caba, Functional properties of chitosan-based films, Carbohydr. Polym., 93, (2013), pp. 339– 346.

11) R. Jayakumar, M. Prabaharan, P.T.S. Kumar, S.V. Nair, H. Tamura, Biomaterials based on chitin and chitosan in wound dressing applications, Biotechnol. Adv., 29, (2011), pp. 322–337.

12) M. Rinaudo, Chitin and chitosan: Properties and applications, Progr. Polym. Sci., 31, (2006), pp. 603-632.

13) W. Arguelles-Monal, F.M. Goycoolea, J. Lizardi, C. Peniche, I. Higuera-Ciapara, Chitin and chitosan in gel network systems, in: H.B. Bohidar, P. Dubin, Y.Osada (Eds.), Polymer gels, Washington D.C.: ACS Symposium Series No. 833, (2003), pp. 102-122.

14) N. Kubota, Y. Eguchi, Facile preparation of water-soluble N-acetylated chitosan and molecular weight dependence of its water-solubility, Polym. J., 29, (1997), pp. 123-127.

15) M. Rinaudo, A. Domard, Solution properties of chitosan, in: G. Skjak-Braek, T. Anthonsen, P. Sandford (Eds.), Chitin and chitosan, Sources, chemistry, biochemistry, physical properties and applications, London and NY: Elsevier, (1989), pp. 71-86.

16) V.G.L. Souza, A.L. Fernando, J.R.A. Pires, P.F. Rodrigues, A.A. Lopes, F.M.B. Fernandes, Physical properties of chitosan films incorporated with natural antioxidants, Ind. Crop Prod., 107, (2017), pp. 565–572.

17) M. Gursoy, I. Sargin, M. Mujtaba, B. Akyuz, S. Ilk, L. Akyuz et al., False flax (Camelina sativa) seed oil as suitable ingredient for the enhancement of physicochemical and biological properties of chitosan films, Int. J. Biol. Macromol., 114, (2018), pp. 1224–1232.

18) J. Hafsa, M. Smach, M.R. Ben Khedher, B. Charfeddine, K. Limem, H. Majdoub, et al., Physical, antioxidant and antimicrobial properties of chitosan films containing Eucalyptus globulus essential oil, Food Sci. Tech., 68, (2016), pp. 356–364.

19) L. Akyuz, M. Kaya, M. Mujtaba, S. Ilk, I. Sargin, A.M. Salaberria, J. Labidi, Y.S. Cakmak, C. Islek, Supplementing capsaicin with chitosan-based films enhanced the anti-quorum sensing, antimicrobial, antioxidant, transparency, elasticity and hydrophobicity, Int J Biol Macromol., 115, (2018), pp,438-446.

20) M. Kaya, S. Khadem, Y.S. Cakmak, M. Mujtaba, S. Ilk, L. Akyuz, et al., Antioxidative and antimicrobial edible chitosan films blended with stem, leaf and seed extracts of Pistacia terebinthus for active food packaging, RSC Advances, 8, (2018), pp. 3941–3950.

21) U. Siripatrawan, W. Vitchayakitti, Improving functional properties of chitosan films as active food packaging by incorporating with propolis, Food Hydrocoll., 61, (2016), pp. 695–702.

22) D. Tsoutsos, D. Kakagia, K. Tamparopoulos, The efficacy of Helix aspersa Muller extract in the healing of partial thickness burns: a novel treatment for open burn management protocols, J. Dermatol. Treat., 20, (2009), pp. 219–222.

23) F. Pons, M. Koenig, R. Michelot, M. Mayer, N. Frossard, The bronchorelaxant effect of helicidine, a Helix pomatia extract, interferes with prostaglandin E2, Pathologie- Biologie (Paris), 47, (1999), pp. 73–80.

24) C. Trapella, R. Rizzo, S. Gallo, A. Alogna, D. Bortolotti, F. Casciano, G. Zauli, P. Secchiero, R. Voltan, HelixComplex snail mucus exhibits pro-survival, proliferative and promigration effects on mammalian Fibroblasts, Sci. Rep., 8(17665), (2018), pp. 1-10.

25) S. Greistorfer, W. Klepal, N. Cyran, A. Gugumuk, L. Rudoll, J. Suppan, J. von Byern, Snail mucus - glandular origin and composition in Helix pomatia, Zoology, 122, (2017), pp. 126–138.

26) J. Newar, A. Ghatak, Studies on the Adhesive Property of Snail Adhesive Mucus, Langmuir, 31(44), (2015), pp. 12155-60.

27) D. Bortolotti, C. Trapella, T. Bernardi, R. Rizzo, Letter to the Editor: Antimicrobial properties of mucus from the brown garden snail Helix aspersa, Brit. J. Biomed. Sci., 73, (2016), pp. 49–50.

28) D.W. Fountain, The Lectin-Like Activity of Helix-Aspersa Mucus, Comp. Biochem. Physiol. B, 80, (1985), pp. 795–800.

29) T. Zhong, L. Min, Z. Wang, F. Zhang, B. Zuo, Controlled self-assembly of glycoprotein complex in snail mucus from lubricating liquid to elastic fiber, RSC Advances, 8, (2018), pp. 13806-13812.

30) M.A. El Mubaraka, F.N. Lamari, C. Kontoyannis, Simultaneous determination of allantoin and glycolic acid in snail mucus and cosmetic creams with high performance liquid chromatography and ultraviolet detection, J. Chromatogr. A, 1322, (2013), pp. 49–53.

31) D.-N. Yu, D. Tian, J.-H. He, Snail-based nanofibers, Mater. Lett., 220, (2018), pp. 5–7.

32) N. Passerini, B. Albertini, S. Panzavolta, L.S. Dolci, Patent n. 102019000004940, Alma Mater Studiorum - Università di Bologna.

33) E96-93 Standard test methods for water-vapor transmission of materials, Annual Book of ASTM Standards, Philadelphia: American Society for Testing and Materials 04(06), (1993), pp. 701-708.

34) O.A. Bozdemir, M. Tutas, Plasticiser effect on water vapour permeability properties of locust bean gum-based edible film, Turk. J. Chem., 27(6), (2003), pp. 773-782.

35) B. Duncan, S. Abbott, R. Roberts, Measurement Good Practice Guide No. 26 Adhesive Tack, National Physical Laboratory Teddington, Middlesex, UK, TW11 0LW, (1999).

36) L. Forte, P. Torricelli, F. Bonvicini, E. Boanini, G.A. Gentilomi, G. Lusvardi, E. Della Bella, M. Fini, E. Vecchio Nepita, A. Bigi, Biomimetic fabrication of antibacterial calcium phosphates mediated by Polydopamine, J. Inorg. Biochem., 178, (2018), pp. 43–53.

37) A. Muxika, A. Etxabide, J.Uranga, P. Guerrero, K. de la Caba, Chitosan as a bioactive polymer: Processing, properties and applications, Int. J. Biol. Macromol., 105, (2017), pp. 1358–1368.

38) K.M. Kim, J.H. Son, K. Sung-Koo, C.L. Weller, A.H. Milford, Properties of Chitosan Films as a function of pH and Solvent Type, J. Food Sci., 71(3), (2006), pp. E119-E124.

39) A. Bégin, M.R. Van Calsteren, Antimicrobial films produced from chitosan, Int. J. Biol. Macromol., 26(1), (1999), pp. 63–67.

40) S. Khoshgozaran-Abras, M.H. Azizi, Z. Hamidy, N. Bagheripoor-Fallah, Mechanical, physicochemical and color properties of chitosan based-films as a function of Aloe vera gel incorporation, Carbohydr. Polym., 87, (2012), pp. 2058– 2062.

41) C. Caner, P.J. Vergano, J.L. Wiles, Chitosan Film Mechanical and Permeation Properties as Affected by Acid, Plasticizer and Storage, J. Food Sci., 63(6), (2006), pp. 1049–1053.

42) D. Lourdin, H. Bizot, P. Colonna, 'Antiplasticization' in starch-glycerol films?, J. Appl. Polym. Sci., 63(8), (1997), pp. 1047–1053.

43) L.F. Boesel, Effect of plasticizers on the barrier and mechanical properties of biomimetic composites of chitosan and clay, Carbohydr. Polym., 115, (2015), pp. 356–363.

44) E. Hernandez, Edible coatings for lipids and resins, in: J.M. Krochta, E.A. Baldwin, M.O. Nisperos-Carriedo (Eds.), Edible coatings and films to improve food quality, Lancaster Pa: Technomic Pub Co. (1994), pp. 279–304.

45) R.J. Samuels, Solid state characterization of the structure of chitosan films, J. Polym. Sci.: Polymer Physics Edition, 19(7), (1981), pp. 1081–1105.

46) H. Saito, R. Tabeta, K. Ogawa, High resolution solid state ^{13}C NMR study of chitosan and its salts with acids: conformational characterization of polymorphs and helical structures as viewed from the conformation-dependent ^{13}C chemical shifts, Macromol., 20, (1987), pp. 2424-2430.

47) J.W. Rhim, S.I. Hong, H.M. Park, P.K. Ng, Preparation and characterization of chitosan-based nanocomposite films with antimicrobial activity, J. Agric. Food Chem., 54, (2006), pp. 5814–22.

48) W. Chang, F. Liu, H.R. Sharif, Z. Huang, H.D. Goff, F. Zhang, Preparation of chitosan films by neutralization for improving their preservation effects on chilled meat, Food Hydrocoll., 90, (2019), pp. 50-61.

49) C. Qiao, X. Ma, J. Zhang, J. Yao, Effect of hydration on water state, gless transition dynamics and crystalline structure in chitosan films, Carbohydr. Polym., 206, (2019), pp. 602–608.

50) M. Bajic, H. Jalšovec, A. Travan, U. Novak, B. Likozar, Chitosan-based films with incorporated supercritical CO2 hop extract: Structural, physicochemical and antibacterial properties, Carbohydr. Polym., 219, (2019), pp. 261–268.

51) M. Lavorgna, F. Piscitelli, P. Mangiacapra, G.G. Buonocore, Study of the combined effect of both clay and glycerol plasticizer on the properties of chitosan films, Carbohydr. Polym., 82, (2010), pp. 291–298.

52) S.F. Wang, L. Shen, Y.J. Tong, L. Chen, I. Y. Phang, P.Q. Lim, T.X. Liu, Biopolymer chitosan/ montmorillonite nanocomposites: Preparation and characterization, Polym. Degrad. Stabil., 90, (2005), pp. 123–131.

53) UNI EN, ISO 10993-5, Biological Evaluation of MEDICAL DEVICES Part 5: Tests for In Vitro Cytotoxicity, (2009).

54) A. Verlee, S.Mincke, C.V. Stevens, Recent developments in antibacterial and antifungal chitosan and its derivatives, Carbohydr. Polym., 164 (2017), pp. 268-283.

55) L.J.R. Foster, J. Butt, Chitosan films are not antimicrobial, Biotechnol. Lett., 33, (2011), pp. 417-421.

Figure captions:

Fig. 1. Appearance of the prepared films. On the right some selected scanning electron micrographs are reported. Bar = 100 micron.

Fig. 2. Stress-strain curves recorded on chitosan films prepared in: a) lactic acid; b) acetic acid; c) S.

Fig. 3. Water Vapor Permeability (***p<0.001, **p<0.01, *p<0.05)

Fig. 4. Adhesive properties of chitosan-based films(***p<0.001, **p<0.01, *p<0.05)

Fig. 5. X-rays diffraction patterns (left) and corresponding IR spectra (right) of chitosan films and lyophilized solution.

Fig. 6. DTG plots recorded on (from top to bottom): films in L, films in A, films in S and lyophilized S.

Fig. 7. Vero cell viability after 48h of incubation with the media containing film components following disks dissolution. Data (mean values ± SD) are relative to the untreated control (set to 100%).

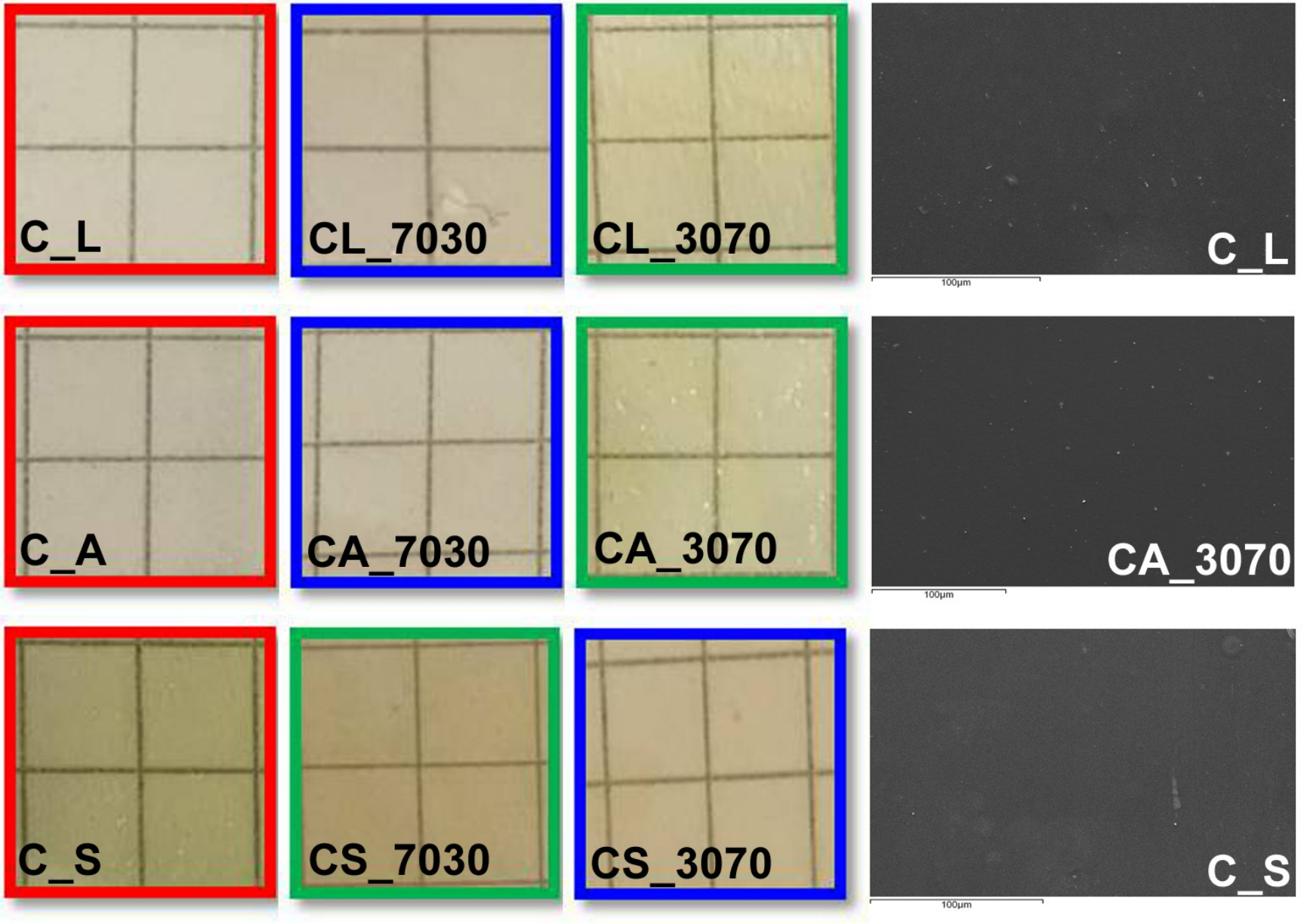
C_L
CL_7030
CL_3070
C_L
100µm
C_A
CA_7030
CA_3070
CA_3070
100µm
C_S
CS_7030
CS_3070
C_S
100µm

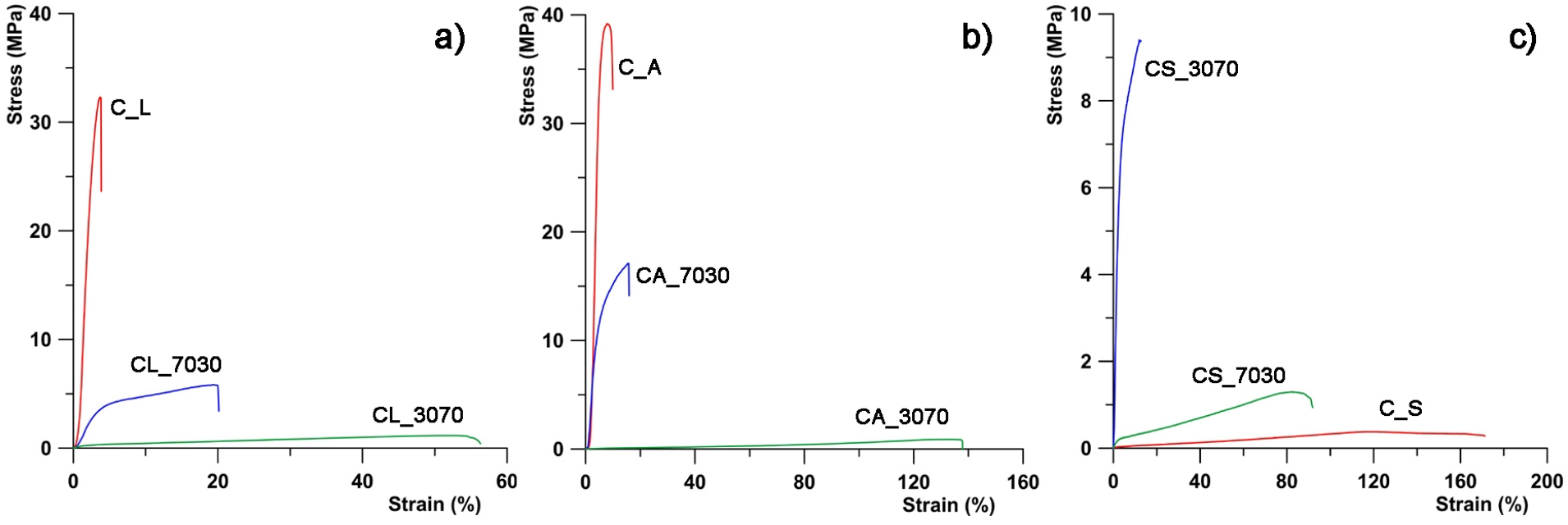
a)
Stress (MPa)
Strain (%)
C_L
CL_7030
CL_3070
b)
C_A
CA_7030
CA_3070
c)
CS_3070
CS_7030
C_S

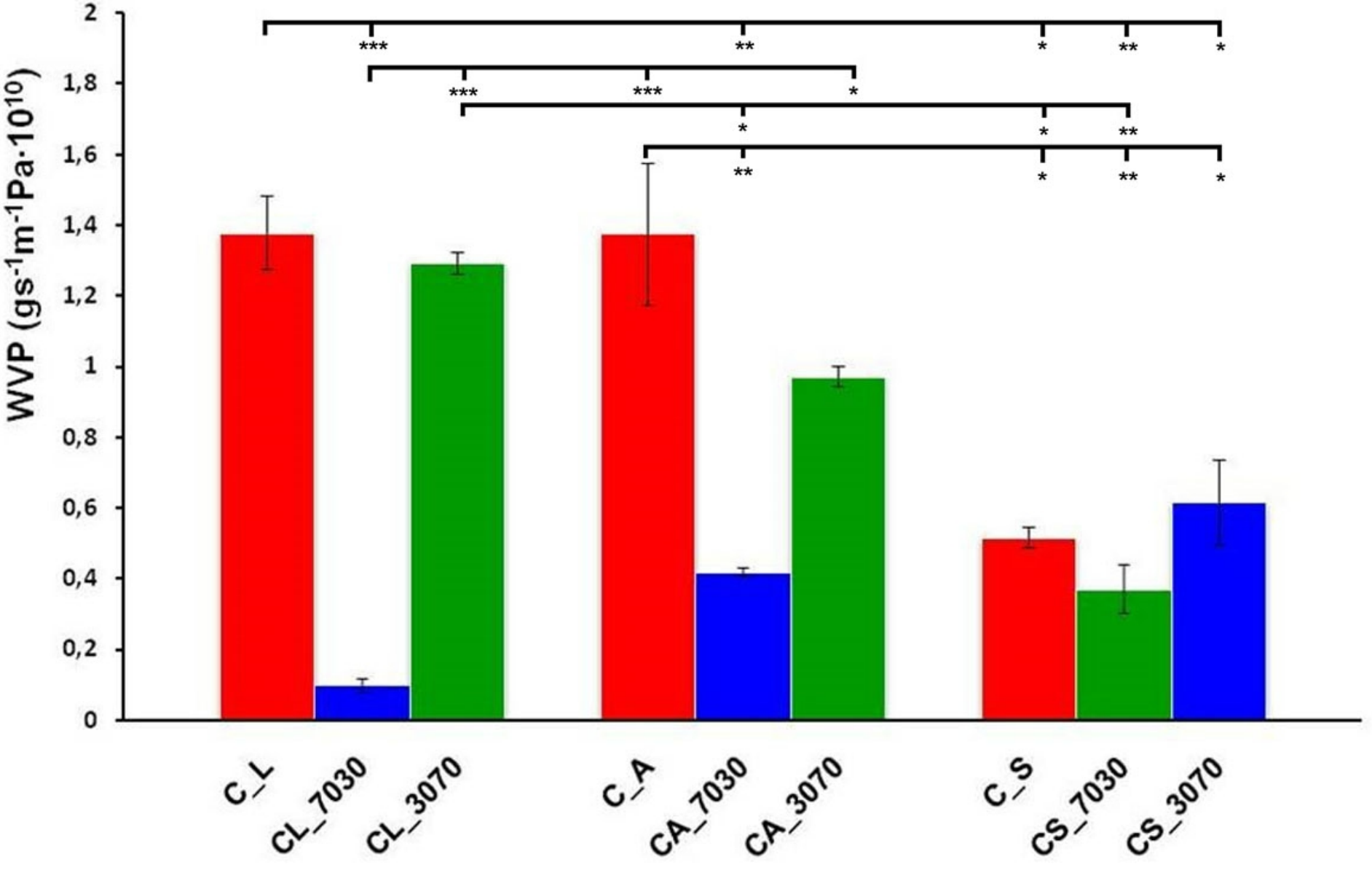
WVP (gs-1m-1Pa·1010)
2
1,8
1,6
1,4
1,2
1
0,8
0,6
0,4
0,2
0
***
**
*
**
*
***
***
*
*
**
**
*
**
*
C_L
CL_7030
CL_3070
C_A
CA_7030
CA_3070
C_S
CS_7030
CS_3070

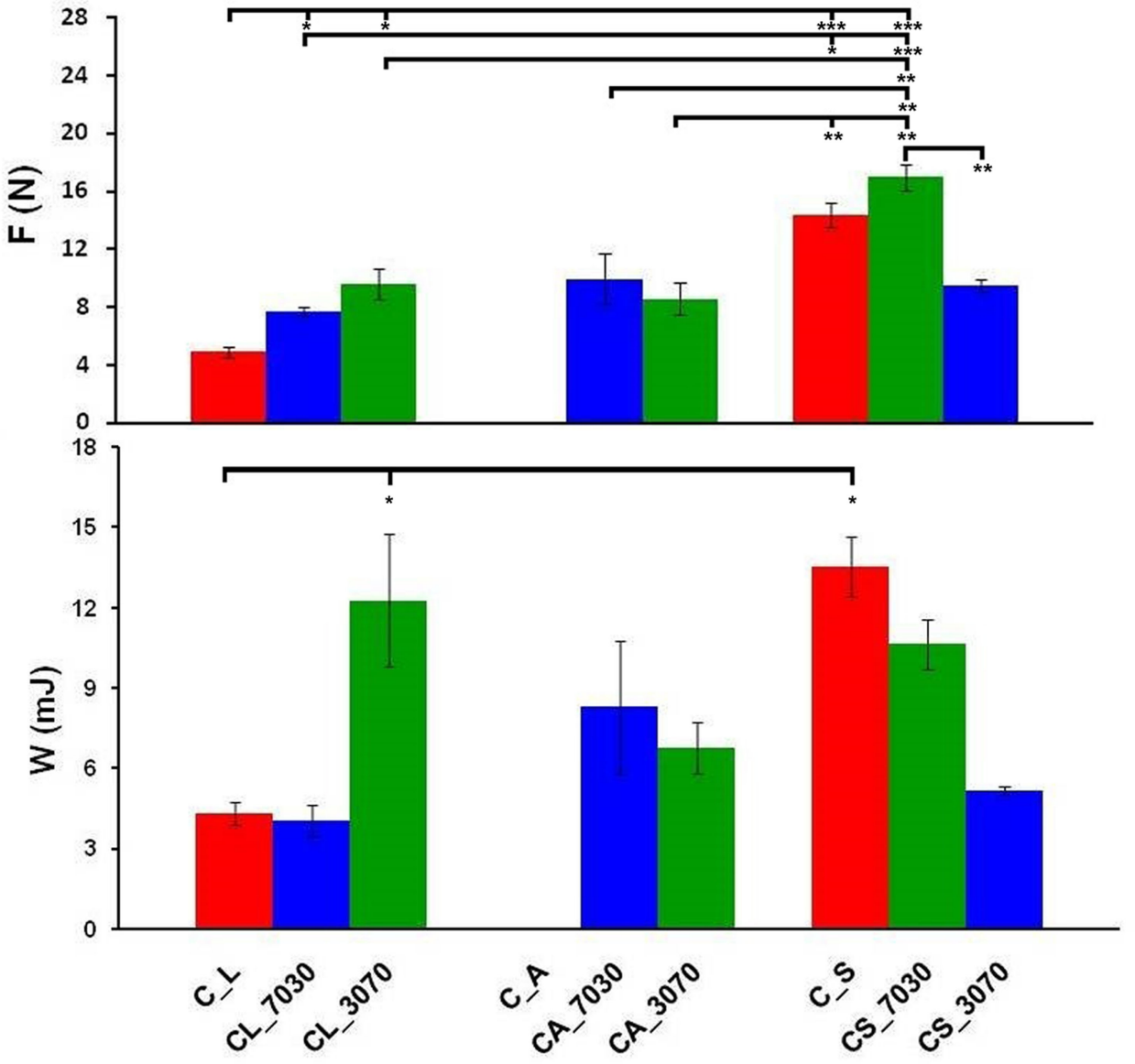
F (N)
28
24
20
16
12
8
4
0
W (mJ)
18
15
12
9
6
3
0
C_L
CL_7030
CL_3070
C_A
CA_7030
CA_3070
C_S
CS_7030
CS_3070

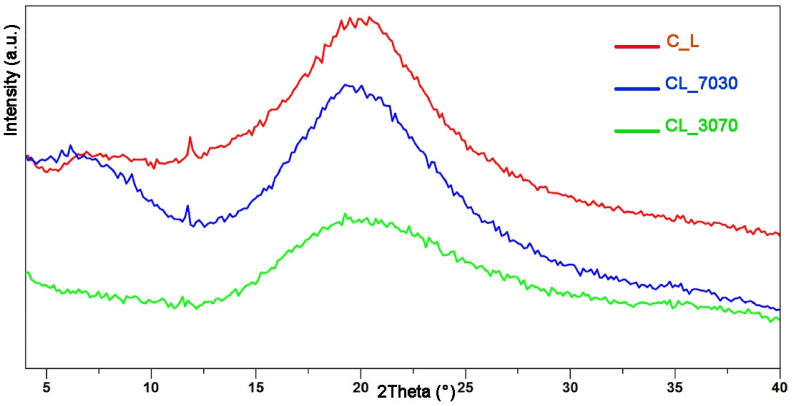
Intensity (a.u.)
C_L
CL_7030
CL_3070
5
10
15
20
25
30
35
40
2Theta (°)

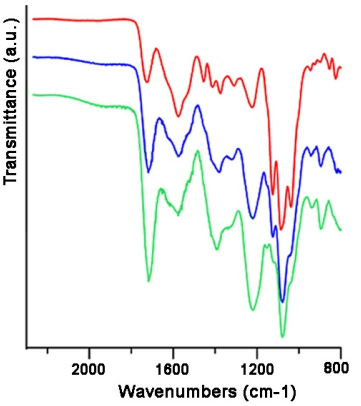
Transmittance (a.u.)
2000
1600
1200
800
Wavenumbers (cm-1)

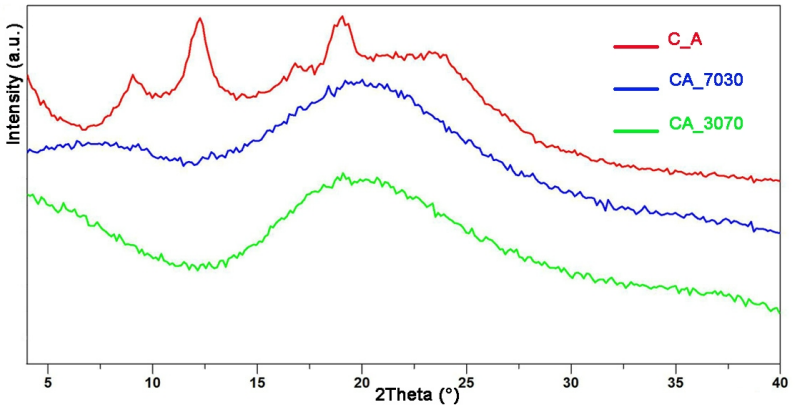
Intensity (a.u.)
C_A
CA_7030
CA_3070
5
10
15
20
25
30
35
40
2Theta (°)

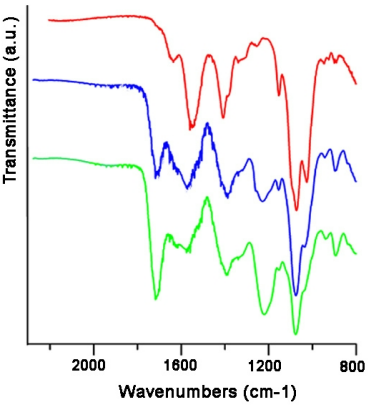
Transmittance (a.u.)
2000
1600
1200
800
Wavenumbers (cm-1)

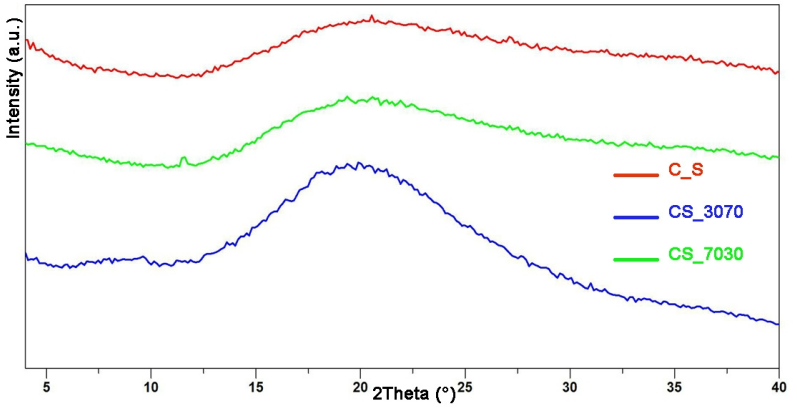
Intensity (a.u.)
C_S
CS_3070
CS_7030
5
10
15
20
25
30
35
40
2Theta (°)

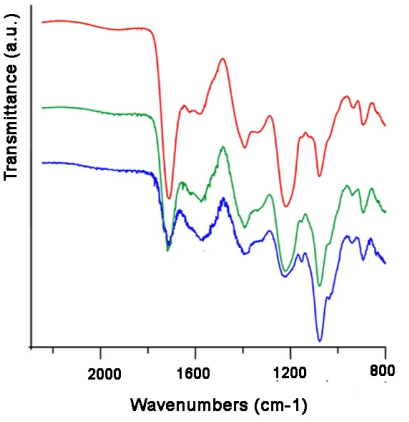
Transmittance (a.u.)
2000
1600
1200
800
Wavenumbers (cm-1)

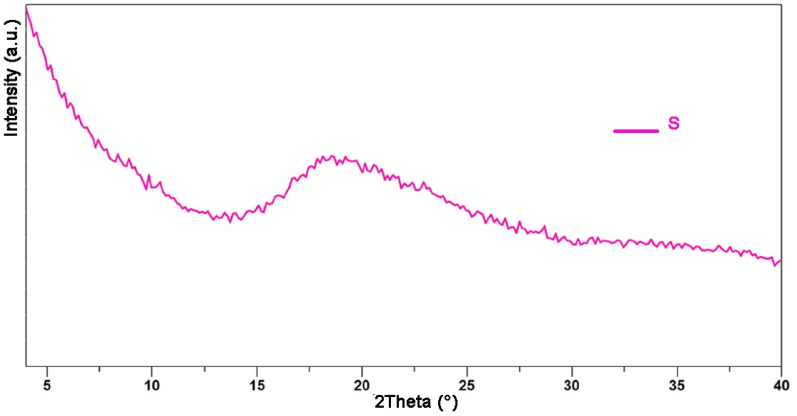
Intensity (a.u.)
S
5
10
15
20
25
30
35
40
2Theta (°)

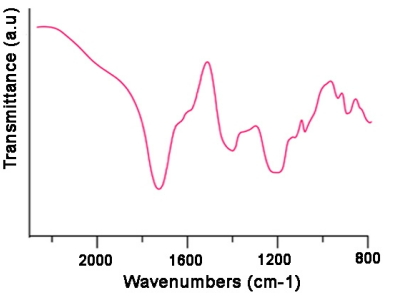
Transmittance (a.u.)
2000
1600
1200
800
Wavenumbers (cm-1)

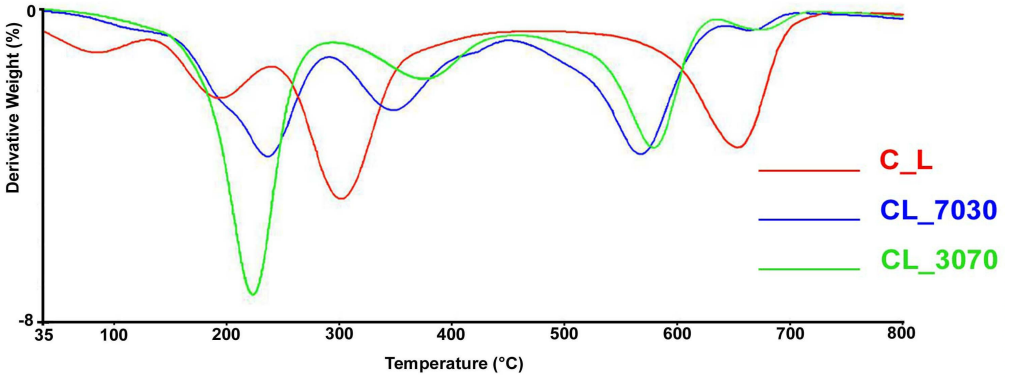
Derivative Weight (%)
0
-8
35
100
200
300
400
500
600
700
800
Temperature (°C)
C_L
CL_7030
CL_3070

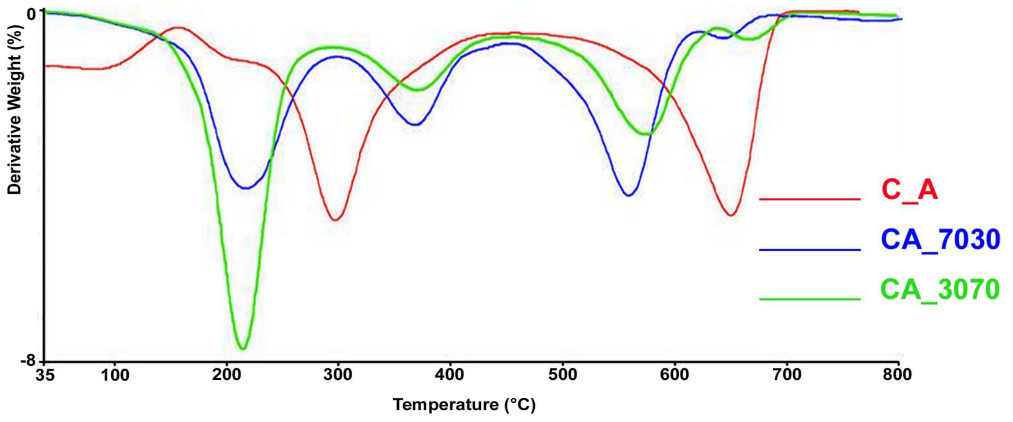
Derivative Weight (%)
0
-8
35
100
200
300
400
500
600
700
800
Temperature (°C)
C_A
CA_7030
CA_3070

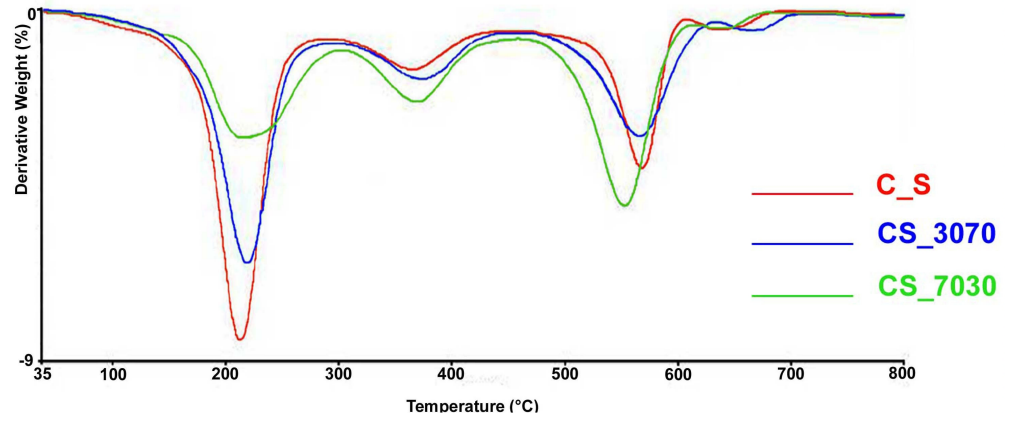
Derivative Weight (%)
0
-9
35
100
200
300
400
500
600
700
800
Temperature (°C)
C_S
CS_3070
CS_7030

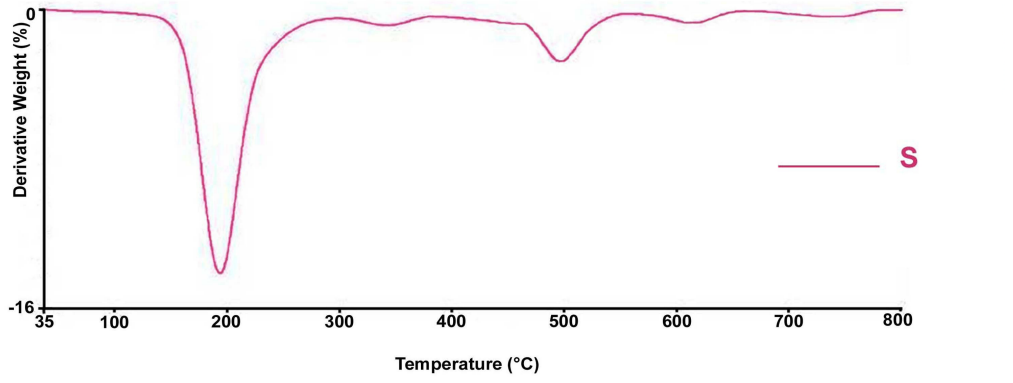
Derivative Weight (%)
0
-16
35
100
200
300
400
500
600
700
800
Temperature (°C)
S

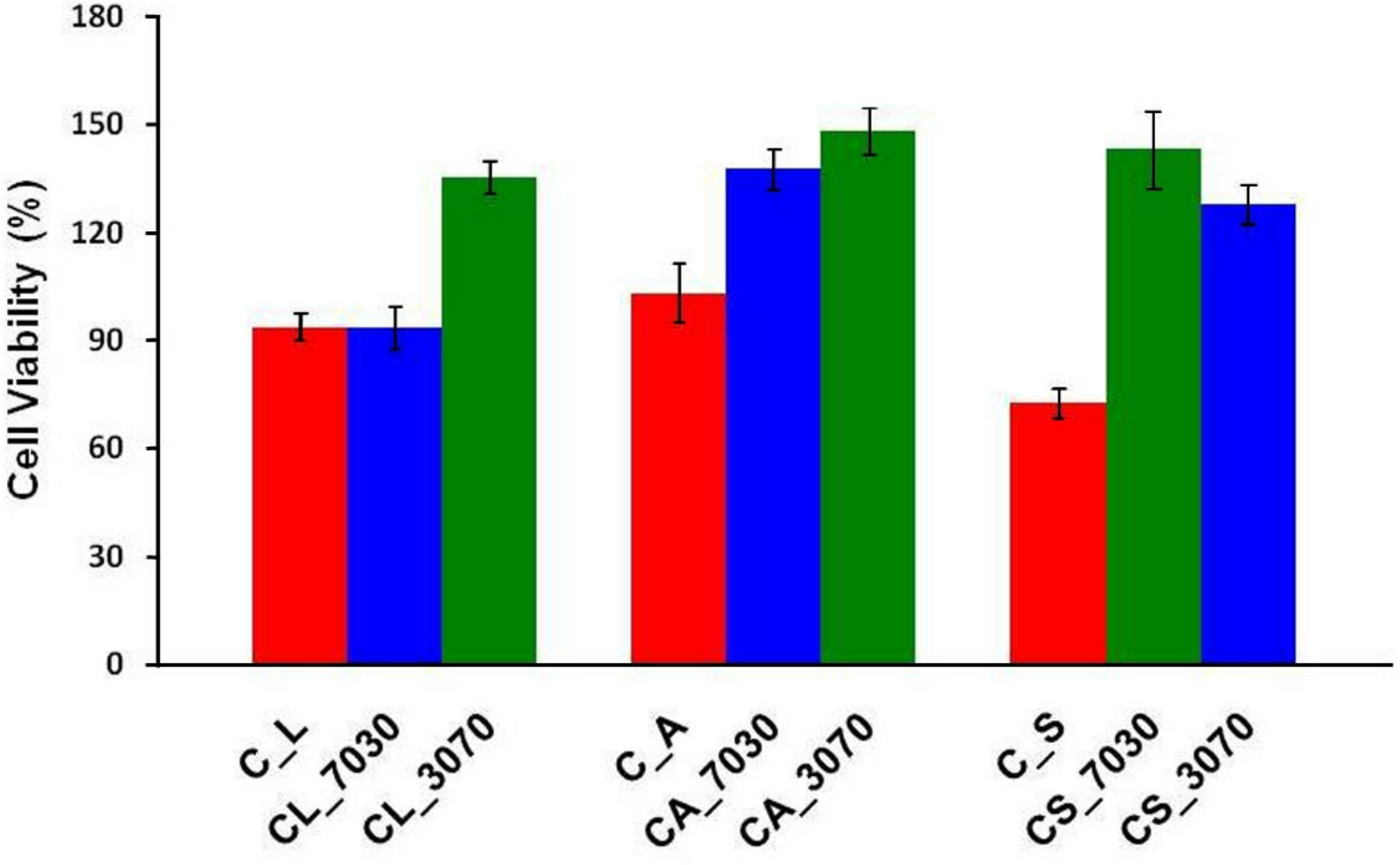
Cell Viability (%)
180
150
120
90
60
30
0
C_L
CL_7030
CL_3070
C_A
CA_7030
CA_3070
C_S
CS_7030
CS_3070

Author Contribution Statement

Maria Francesca Di Filippo: Data curation, Formal analysis, Investigation, Roles/Writing – original draft;

Silvia Panzavolta: Conceptualization, Methodology, Project administration, Supervision, Roles/Writing – original draft, Writing – review & editing;

Beatrice Albertini: Methodology, Roles/Writing – original draft, Writing – review & editing;

Francesca Bonvicini: Data curation, Formal analysis, Investigation;

Giovanna Gentilomi: Resources

Ramona Orlacchio: Data curation, Formal analysis, Investigation;

Nadia Passerini: Resources, Supervision;

Adriana Bigi: Supervision, Writing – review & editing;

Luisa Stella Dolci: Conceptualization, Resources, Validation.

FUNCTIONAL PROPERTIES OF CHITOSAN FILMS MODIFIED BY SNAIL MUCUS EXTRACT

Maria Francesca Di Filippo[a], Silvia Panzavolta*[a], Beatrice Albertini[b], Francesca Bonvicini[c], Giovanna Gentilomi[c], Ramona Orlacchio[a], Nadia Passerini[b], Adriana Bigi[a], Luisa Stella Dolci[b]

[a]Department of Chemistry "G. Ciamician", University of Bologna, Via Selmi 2, 40126, Italy;

[b]Department of Pharmacy and BioTechnology, University of Bologna, Via S. Donato 19/2, 40127, Italy;

[c]Department of Pharmacy and Biotechnology, University of Bologna, Via Massarenti 9,40138, Italy

Specification	Values	Measure Units	Method
Aspect	Clear		
smell	Odorless		
Color	Pale yellow		
pH	2.9		
Density	1.0-1.04	g/ml	
Dry residual	5 %	M/V	M.I.M 180305/L Rev. 0:2005
Minerals (K, Ca, Na)	538	mg/L	M.I.M 110315/C Rev. 0:2005
Heavy metals	absent		
Proteins	80 - 120	mg/L	Bradford proteins assay method
Glycolic acid	60-80	mg/L	J. Chrom. A. 1322, pp 49-53, 2013
Allantoin	100-130	mg/L	J. Chrom. A. 1322, pp 49-53, 2013
Iron	3	mg/L	M.I.M 111010/C Rev. 0:2010
Citric acid	<0.1	mg/L	M.I.M 150212/A Rev. 0:2012
Ascorbic acid	<0.1	mg/L	M.I.M 150212/A Rev. 0:2012
Antiprotease	1.3	mg/L	M.I.M 0112016/A Rev. 0:2016
D-lactic Acid	<10	mg/L	M.I.M 0112016/A Rev. 0
L-lactic Acid	<10	mg/L	M.I.M 0112016/A Rev. 0
Sodium benzoate	<0.002%	m/m	M.I.M 150212/A Rev 0:2012
Collagen	2-60	mg/L	M.I.M 0112016/H Rev. 0:2016
Gram +	<10	UFC/g	UNI-EN ISO6888-1:2004
Gram -	<10	UFC/g	ISO 16649-2:2001
Fungi	<10	UFC/g	NFV08-059:2002

Table S1: Characterization of snail mucus obtained from Helix Aspersa Muller by means of MullerOne technology. Analyses were obtained by the supplier. The chemical and microbiological parameters evaluated are among those suggested for snail mucus characterization, as reported in http://www.mullerone.com/it/en/our-slime-helix.